Energy & Environmental Science

Accepted Manuscript

ROYAL SOCIETY OF CHEMISTRY

www.rsc.org/ees

Evaluation of sulfur spinel compounds for multivalent battery cathode applications

Miao Liu[1], Anubhav Jain[1], Ziqin Rong[2], Xiaohui Qu[1], Pieremanuele Canepa[3], Rahul Malik[2]

Gerbrand Ceder[2,3,4] and Kristin A. Persson[1,4*]

[1]Electrochemical Technologies Group, Lawrence Berkeley National Laboratory, CA 94720, USA

[2]The Department of Materials Science and Engineering, Massachusetts Institute of Technology, Cambridge MA 02139, USA

[3]Materials Sciences Division, Lawrence Berkeley National Laboratory, Berkeley, California 94720, USA

[4]Department of Materials Science & Engineering, University of California, Berkeley, CA 94720-1760, USA

Abstract

The rapid growth of portable consumer electronics and electric vehicles demands new battery technologies with greater energy stored at a reduced cost. Energy storage solutions based on multivalent metals, such as Mg, could significantly increase the energy density as compared to lithium-ion based technology. In this paper, we employ density functional theory calculations to systematically evaluate the performance, such as thermodynamic stability, ion diffusivity and voltage, of a group of 3*d* transition-metal sulfur-spinel compounds (21 in total) for multivalent cathode applications. Based on our calculations, Cr_2S_4, Ti_2S_4 and Mn_2S_4 spinel compounds exhibit improved Mg^{2+} mobility (diffusion activation energy < 650 meV) relative to their oxide counterparts, however the improved mobility comes at the expense of lower voltage and thereby lower theoretical specific energy. Ca^{2+} intercalating into Cr_2S_4 spinel exhibits a low diffusion activation barrier of 500 meV and a voltage of ~2V, revealing a potential cathode for use in Ca rechargeable batteries.

* Corresponding author email: kapersson@lbl.gov

Broader Context

The high cost and limited volumetric capacity of the lithium ion battery (LIB) technology challenges its application in transportation applications. Multivalent batteries, such as those utilizing Mg^{2+} or Ca^{2+} as the working ions, are promising candidates for beyond LIB technology due to the potential increase in volumetric capacity and reduced cost. In the present work, we systematically evaluate the performance of a group of sulfur spinel compounds as potential cathode materials based on first-principles calculations. We find that - unlike most oxide materials which generally exhibit sluggish mobility of the multivalent cation - sulfur spinels provide a better chemical framework for multivalent mobility. Screening the set of cathode materials on voltage, capacity, thermodynamic stability as well as ion mobility, $MgCr_2S_4$, $MgTi_2S_4$, $MgMn_2S_4$ and $CaCr_2S_4$ emerge as the most promising for multivalent cathode applications amongst the 3*d* transition–metal sulfur spinel compounds. We also present several general trends and design insights extracted from our evaluation for this category of materials.

Introduction

High-energy density rechargeable batteries have enabled a revolution in consumer electronic devices, and recently the technology is contributing to emerging markets such as electric vehicles and load balancing of intermittent renewable power sources. Multivalent batteries, such as those utilizing Mg^{2+} as the working ion, have the potential to outperform current battery technologies due to their increased theoretical volumetric capacity and improved safety[1–3]. One exciting possibility is to use Mg metal directly as the battery anode, taking advantage of its fairly low reduction potential of -2.37 V (*vs* SHE) and good metal plating morphology (less dendrite formation) upon deposition.[4,5] This alone would improve

the volumetric capacity of the anode by over 4 times, from the ~800 mAh/cc in graphite[3–5] used today in Li-ion batteries to 3833 mAh/cc for metallic Mg. Furthermore, Mg^{2+} carries two charges with a similar ionic radius compared to a Li^{+} ion. Therefore, the theoretical cathode capacity can, depending on the specific chemistry, potentially be doubled at the same volume[6,7]. In addition, the natural abundance of multivalent elements, such as Mg and Ca, is significantly higher than that of Li (the atomic abundance of Mg is ~10^4 times larger than Li in earth crust), guaranteeing sufficient supply even for multi-fold increases of the energy storage market.

However, multivalent energy storage is still a nascent technology. One major limitation of the proposed multivalent battery systems is the generally poor diffusivity of the multivalent ion in most known cathode materials. Materials known to be viable Li cathodes, such as spinel oxides, exhibit impeded ion diffusivity when repurposed for multivalent species.[7–9] Furthermore, in contrast to Li-ion batteries, the transport properties of Mg intercalation in electrode materials is impacted by complex Mg desolvation mechanisms from the bulk electrolyte to the electrode surface followed by bulk diffusion.[5,10,11] The availability of Mg near the surface electrode is ultimately set by the complex thermodynamic of the liquid electrolyte solutions as observed by Canepa *et al.*[12]

To enable reasonable ion mobility, the activation barrier for ion migration should be <~600 meV,[9] although particle size and, to some degree, temperature[13] can be used to mitigate the inherent low bulk mobility. Using high-throughput first-principles calculations, Liu *et al.* recently evaluated a matrix of spinel oxides[7] and observed that the Mg^{2+} activation barrier in Mn_2O_4, Co_2O_4 and Cr_2O_4 ranges between 650-850 meV in the dilute limit. Further first-principles calculations from Gautam *et al.* indicate that the situation is similar for δ-V_2O_5, in

which the activation energy of Mg^{2+} diffusion ranges between 600-800 meV.[9,14] Based on these results, the performance of Mn_2O_4 and Co_2O_4 spinel compounds and layered δ-V_2O_5 will be limited by Mg^{2+} diffusivity[15].

We note that one recent experimental work demonstrated highly reversible and extensive intercalation of Mg into the tetrahedral sites of Mn_2O_4 spinel, but only achieved a low degree of intercalation (3 at% Mg in the discharged state) when paired with a non-aqueous electrolyte,[8,12] consistent with the kinetic limitations predicted by theory (activation barrier of ~800meV in cation dilute limit).[7] Indeed, one might intuitively expect that the multivalent elements, due to their higher charge compared to Li^+, will form stronger bonds with the oxygen anion lattice and will hence generally exhibit larger activation barriers for ionic mobility. However, recent work compared the mobility of multivalent intercalating ions in several different oxide frameworks and found the diffusion barrier to be highly dependent on the intercalant site preference to the diffusion path topology of the host structure.[9] Thus, tailoring the structure carefully to the migrating ion size and electronic structure provides one of the most important controls for mobility. Another design control can be leveraged by tuning of the chemistry rather than the structure. In contrast to oxide materials, previous findings hint that sulfides may exhibit improved Mg ion diffusivity. Aurbach *et al.* reversibly inserted Mg into the anionic framework of Chevrel Mo_6S_8, obtaining a capacity of ~70 mAh/g for more than 600 cycles[1]. Liang *et al.* reported that highly exfoliated graphene-like MoS_2 accompanied by a nano-sized Mg anode can deliver ~170 mAh/g capacity and 1.8V voltage for over 50 cycles[16]. Furthermore, the Mg^{2+} ionic conductivity can be optimized with the expanded interlayer spacing[17]. In addition, Tao *et al.* demonstrated reversible Mg intercalation/deintercalation in TiS_2 with tube morphology[18]. Recent theoretical work predicts low Mg mobility, in spinel and layered O1 type TiS_2

(barriers corresponding to 860meV and 1160meV, respectively), but suggests that strain engineering could be used to enable more facile Mg intercalation.[19] Motivated by the above-mentioned studies of sulfides, we here systematically evaluate 21 sulfur spinel compounds to uncover their potential for multivalent cathode applications and compare these properties against those previously obtained for oxides. It is expected that the set will exhibit lower voltage as compared to the oxide counterparts, however, the goal of our work is to evaluate the benefits as well as drawbacks in tuning chemistry through the anion framework as well as to suggest improved cathodes as compared to the Chevrel phase. Properties such as insertion voltage, capacity, stability and intercalant mobility are evaluated to help select the most promising candidate materials for experimental synthesis and characterization. Moreover, we uncover the general trend and diffusion mechanism in this category of compounds, and provide a guide for future material synthesis and design.

Results

Spinel compounds belong to space group $Fd\bar{3}m$ with the general formula AB_2X_4. The anion 'X' can be oxygen to form oxide spinels or divalent S or Se ions to form thiospinels. Within the spinel crystal structure, the cation 'B' is octahedrally coordinated by anion X, and these octahedra share edges and extend in space such that there exist 3D diffusion channels (Fig 1). In a normal spinel, cation 'A' occupies the tetrahedral sites to form the $Fd\bar{3}m$ symmetry.[20,21] Apart from the tetrahedral site that is occupied by cation 'A', there also exist face-sharing octahedral sites located between the tetrahedral sites. In some materials, cation 'A' occupies these octahedral sites rather than the typical tetrahedral sites, either due to the 'A' cation naturally favoring an octahedral environment or due to limited availability of tetrahedral sites when the concentration of 'A' is high. In this case, the crystal structure can be categorized into a rocksalt-like geometry belonging to space group *Imma* as shown

in Figure 1(b).[22,23] For example, Ca prefers octahedral sites in Mn_2O_4 host structures;[7] and excessive intercalation of Li ions into Mn_2O_4 spinel host will also push the tetrahedral Li into the octahedral sites and form rocksalt $LiMnO_2$[24]. The diffusion path for the 'A' cation alternates through tetrahedral and octahedral sites along zigzag-shaped paths as illustrated in Figure 1(c).[9] In this paper, we systematically evaluate the performance of sulfur spinels (formula AB_2S_4) as multivalent cathode materials, selecting 'A' atoms from the set {Mg, Ca, Zn} and 'B' atoms as redox-active 3*d* transition metals from set {Ti, V Cr, Mn, Fe, Co, Ni}, totaling 21 combinations.

First, we evaluated the thermodynamic stability of compounds within the sulfur spinel family. The thermodynamic stability of a material is defined as the driving force to decompose a compound into a combination of the most stable compounds in its corresponding chemical system[9]. To determine the appropriate set of stable compounds for comparison as well as their energies, we combine our first-principles calculation results with the comprehensive data available in the Materials Project[25]. The thermodynamic stability of a target spinel phase was estimated by comparing its formation energy against the convex hull of ground state energies in the relevant portion of the phase diagram, which represents the driving force for decomposition and which we refer to as "energy above hull".[26–28] A high energy above hull indicates that a material is thermodynamically unstable, and serves as an indicator for synthesizability as well as the likelihood for degradation upon cycling.[29]

Figure 2 plots the energy above hull for fully discharged and fully charged phases for each compound in sulfur spinel family. The thermodynamic stability results suggest that both Ti_2S_4 and Mn_2S_4 spinel structures represent relatively stable empty hosts for cation

intercalation. The three compounds V_2S_4, Cr_2S_4 and Ni_2S_4, exhibit moderate energy above hull values of approximately 70 meV/atom, and are less stable than the Ti- and Mn-containing phases but still within the energy scale of common metastable compounds. Amongst the 21 compounds, in the discharged phase, ACr_2S_4 and ATi_2S_4 are the most stable compounds with A={Ca, Mg, Zn}. $MgCr_2S_4$ and $ZnCr_2S_4$ possessing the lowest energy above hull and hence are likely accessible through direct synthesis. $MgMn_2S_4$ and $MgTi_2S_4$ spinel in the discharged phase have fairly low above hull energies as well, whereas both V_2S_4 and Fe_2S_4 spinel compounds fall into the unstable range with large above hull energies (> 85meV/atom, c.f. Figure 2).

A priori it is unknown whether a cation 'A' in AB_2S_4 spinels occupies the tetrahedral or the octahedral site, wherefore we evaluated the thermodynamic stabilities for both situations. Site preference is assessed by placing the multivalent intercalant 'A'={Ca, Mg, Zn} on either the tetrahedral or octahedral sites and evaluating the difference in energy. These site energy differences are plotted in Figure 2 as a function of chemistry. Both the size and electronic structure can affect the A cation's site preference. Ca compounds normally prefer the rocksalt-type structure in which they are octahedrally coordinated. The site energy difference is approximately 500 meV for Mn_2S_4 and Cr_2S_4 and approximately 600-650 meV for other compounds. In sulfur spinels, the preference of octahedral sites for the Ca^{2+} ion is due to its larger ionic size in accordance with Pauling's rule[30]. Mg^{2+} has a smaller ionic size relative to Ca^{2+}, and the ratio between the Mg^{2+} and S^{2-} ionic radii is ~0.4, falling into a range that favors both octahedral and tetrahedral environments.[30] Therefore, amongst the intercalant species {Ca, Mg, Zn}, Mg is the most flexible in terms of cation site preference and displays the smallest site energy difference. In $MgMn_2S_4$ and $MgTi_2S_4$, the site energies for Mg between the two types of sites are almost equal, although for $MgCr_2S_4$ and $MgCo_2S_4$

there is a stronger preference for the tetrahedral site (which is ~400 meV and ~500 meV lower than octahedral site, respectively). At compositions AB_2X_4, for octahedral A cations only half of the sites are filled and hence, there is a choice of which sites to occupy. We investigated nine different randomly chosen, but evenly distributed, Mg cations among the available octahedral sites in TiS_2, as a representative case. We estimate that the choice of octahedral site configuration may modify the site energy by less than ~20meV, which is obtained from an extensive investigation of the Mg site energies for both octahedral and tetrahedral site configurations in TiS_2.[31] The Zn^{2+} ion generally prefers tetrahedral sites as exhibited by the ~1050 meV (calculated from ~150 meV/atom E above hull energy) difference in stability as compared to the rocksalt-like phase. Zn prefers four-coordinated tetrahedral environments[32] because the Zn^{2+} ion, with an electronic structure of [Ar]$3d^{10}$, has ten electrons outside the argon shell that completely fill the 3*d* orbitals, leaving only the empty 4s and 4*p* orbitals to form sp^3 hybridization. In the rest of our work, we adopt the most stable site for the respective mobile cation in the discharged state.

In addition to determining structure and stability, the cation site preferences can be related to cation mobility. The diffusion path in spinel structures traverses the tetrahedral as well as the octahedral sites[9]; thus, the energy difference represents a minimum value for the activation barrier and low site energy *differences* indicate higher cation mobility. For example, Zn-containing compounds are not preferred because a 1050 meV site energy difference implies a migration energy barrier of at least 1050 meV. Therefore, we focus our attention to compounds with low site energy differences to maximize the chance of finding a host enabling facile MV ion diffusion.

Combining the assessments of thermodynamic stability and the minimum activation barriers of sulfur spinels, Cr_2S_4, Ti_2S_4 and Mn_2S_4 emerge as the top three candidates. To obtain more accurate diffusion activation barriers for these materials, we performed nudged elastic band (NEB) calculations to compute the energy along the migration path for Cr_2S_4, Ti_2S_4 and Mn_2S_4 in the limit of dilute cation insertion (Figure 3). Compounds that exhibit reasonable cation mobility (Table 2) under these assumptions include: Mg in Mn_2S_4 (515 meV), Ca in Cr_2S_4 (542 meV), Mg in Cr_2S_4 (567 meV), and Mg in Ti_2S_4 (615 meV). Other combinations exhibit much larger activation barriers, up to ~1500 meV for Zn^{2+} migration in Cr_2S_4. We note that these findings are in very good qualitative agreement with the estimations based only on site energy difference (Figure 3(d)). While the site energy differences do not fully determine the migration barrier, one can use it as an indicator to screen out compounds based on a lower estimate of the activation energy. In particular, the activation energy barrier in spinels equals the site energy difference plus the additional energy needed for the cation to pass through an intermediate transition state composed of a narrow, triangular aperture of three sulfur atoms. This intermediate state corresponds to the two activation barrier maxima at the ~25% and ~75% points along the diffusion path in Figure 3(a-c)[9]. The variable energy in passing through this triangle aperture adds an additional energy cost of ~0-600meV, and elevates the activation barrier for compounds which exhibit small site energy differences [Figure 3(d)].

In addition to stability and diffusion, we plot in Figure 4(a) the calculated average voltage *vs.* the gravimetric capacity for the full intercalation reaction of B_2S_4 +A -> AB_2S_4 for the intercalants A = {Mg, Ca Zn, Y, Al} and redox active transition metals B = {Ti, V, Cr, Mn, Fe, Co, Ni}. We find, not surprisingly, that the average voltage of sulfur spinels is significantly lower than that of oxide spinels; for example, Ca intercalation in oxides occurs in a range of

2.7-4.0V (excluding Ti_2O_4, which has an average voltage of 1.5V)[7], whereas the average voltages of non-Ti sulfur spinel compounds fall in the range of 1.2-2.0V. Similarly, Mg and Zn intercalation in sulfide spinels occurs at approximately 1.5V below their oxide counterparts. This is consistent with the effect of the anion potential on Li-insertion reactions clarified in early first-principles work on lithium cathodes.[33]

The detailed variation of intercalation voltage versus redox metal species is plotted in Figure 4(b). The differences in voltage between insertion cations stay roughly constant regardless of the redox metal choice: Ca intercalation occurs ~0.2V higher than that of Mg, and Mg intercalation occurs ~0.5V higher than that of Zn. This voltage trend is consistent with, but less pronounced than, the aqueous electrochemical series of {Ca, Mg, Zn}, i.e., $E^0_{Ca(aq)}$=-2.86V, $E^0_{Mg(aq)}$=-2.37V and $E^0_{Zn(aq)}$=-0.76V. Similarly, regardless of the choice of active cation {Mg, Ca, Zn}, the qualitative trend versus redox element follows a similar pattern: Cr_2S_4 host structures provide the maximum voltage and Ti_2S_4, Mn_2S_4 and Ni_2S_4 exhibit relatively lower voltage. The voltage profile of the sulfide spinels can be related to the corresponding change in electronic configuration between the charged and discharged states. For example, Cr exhibits a high voltage because the discharged state, Cr^{3+}, has a very stable electronic configuration (d^3, corresponding to half-filled t_{2g} orbitals) whereas the charged state, Cr^{4+}, has an unstable electronic configuration (d^2, which tends to oxidize further to d^0, corresponding to Cr^{6+}). Conversely, the "low voltage" metals exhibit more stable electronic configurations in the charged state. For example, Ti^{4+}, Mn^{4+} and Ni^{4+} are very stable, containing, respectively, d^0, half-filled and filled t_{2g} states. In these instances, intercalation adds an electron that results in a less stable electronic arrangement for the host metal, sometimes (in the case of Ni and perhaps Mn) filling an antibonding orbital, which results in decreased stability.

In addition to the lower voltage, the gravimetric capacities of sulfur spinel compounds are approximately 30% lower than their oxide counterparts due to the added mass of the S ion. Considering the reductions in both voltage and capacity, the specific energy of the sulfur spinel compounds is on the order of ~400 Wh/kg. However, it is possible that sulfur-based compounds, with their improved intrinsic bulk cation mobility and less need (presumably) for electronically conductive coatings, could achieve a higher fraction of their theoretical energy density, and thus higher practical energy densities. It should also be noted that such systems represent potentially better performance than that demonstrated from the Chevrel phase,[1] which is often taken as a point of reference for multivalent cathode compounds as the only to date known cathode which reversibly cycles Mg at room temperature.[1]

Considering all the properties evaluated (Table 1), Mg or Ca in a Cr_2S_4 spinel host are found to be the most promising cathode materials due to their good mobility and acceptable voltage. Mg in Mn_2S_4 and Ti_2S_4 may also be worthwhile systems to study on the basis of the favorable cation mobility.

Discussion and conclusion

In this paper, we used first-principles calculations to evaluate the electrochemical properties of multivalent intercalation in sulfur spinel compounds. To exemplify our approach, we include a comparison between our DFT calculations and available experimental results for verified Mg intercalation in Table 2. Here we also include new benchmarking results on the Chevrel Mo_6S_8 phase (see Methodology Section) which demonstrates a very low migration barrier of 360 meV for Mg^{2+} in the dilute (charge) cation

limit, in agreement with its demonstrated excellent intercalating properties as shown by the Aurbach group[1].

Based on our evaluations of compound stability, cation activation energy, voltage and capacity, $MgCr_2S_4$, $MgTi_2S_4$, $MgMn_2S_4$ and $CaCr_2S_4$ spinel compounds hold the most promise for multivalent cathode applications amongst the 3*d* transition–metal sulfur spinel compounds. The calculation method we adopt has been proven to be reliable for evaluating electrochemical intercalation in Mn oxide spinel[7,8] and Chevrel Mo_6S_8 (see benchmark calculations in the Methodology Section) [11,34] and most recently in thiospinel TiS_2 [31](see Table 2).

We identified several combinations of active cation and redox metal ions that exhibit excellent thermodynamically stability in both the fully charged as well as the fully discharged states. Furthermore, in the sulfur spinel structure, we found that Zn tends to prefer tetrahedral sites, Ca tends to prefer octahedral sites, and Mg shows similar preference for octahedral and tetrahedral sites. These results, which are related to the electronic configuration of the active cations and their ionic radii, not only determine the preferred cation sites, but also set bounds on the intrinsic mobility of the different host/intercalant combinations. Our results indicate that for the spinel structure, it is feasible to filter out materials with poor cation mobility using site energies alone. However, to identify compounds with promising cation mobility the minimum energy along the diffusion paths needs to be evaluated. Activation barrier calculations using the nudged elastic band method found four compounds with acceptable cation mobility: $MgTi_2S_4$, $MgCr_2S_4$, $MgMn_2S_4$, and $CaCr_2S_4$. It is noticeable that there is a distinctive difference between this work and a recent report by Emly *et al.*[19] regarding the activation energy barrier for Mg

diffusion in Ti_2S_4 at dilute concentrations, e.g. ~600meV reported here as compared to 860meV in Ref [19]. We believe that the discrepancy is primarily caused by the difference in equilibrium lattice parameter used in the NEB calculations – in this work, the relaxed discharged material (e.g. the calculation cell is relaxed with intercalant) is employed in the NEB calculations instead of the using that of the end member (empty) charged structure. Indeed, Emly *et al.* finds that the activation energy can be dramatically modified by the volume change[19] and even a small amount of well-distributed cations can expand the volume of host significantly. Hence, our results are actually in good agreement with Emly *et al*. considering the effect of the intercalant-induced volume expansion. Although our calculations indicate that sulfides may be advantageous compared to oxides in terms of diffusivity, sulfur spinel compounds exhibit lower intercalation voltages by more than 2V and lower gravimetric capacity. For a particular intercalant, the choice of redox metal affects the voltage by ~0-0.7V, which can largely be explained by considering the electron configuration of the transition metal. The low voltage of this series of compounds also hints at a possible platform for batteries with aqueous electrolytes, although we anticipate that stability of sulfides in an aqueous environment would present additional challenges.[35]

In general, intercalant mobility is mainly determined by three factors: (1) connectivity between sites; (2) sizes of the diffusion channel/cavity and intercalant; (3) and interaction strength between the intercalant and host structure. The site connectivity divide cathode materials into 1D, 2D or 3D intercalation topology, which in turn affects the diffusion behavior of a material dramatically as, in principle, a well-distributed diffusion network should facilitate mobility by providing improved tolerance towards defects and changes in lattice parameters.[13,36] Moreover, the channel size should be large enough to accommodate the intercalant. Finally, high mobility is facilitated by weak interaction between the

intercalant and host anion lattice. In sulfide spinels, the 3D diffusion channels and expanded volume (the latter as compared to oxide spinels), at least the first two criteria are satisfied. Meanwhile, the ionic interaction between intercalant and host framework is likely reduced considering the longer 'A'-S bond (than 'A'-O bond) and the lower electronegativity of S^{2-} as compared to O^{2-}. Hence, for sulfide systems, we surmise that facilitated intercalant mobility can be achieved through i) a weakening of ionic bonds between the migrant ions and the host structure and ii) a moderate increase of diffusion channel size. Our systematic study allows for a rigorous quantification in the gain in mobility going from S^{2-} instead of O^{2-}, for the same structure. Indeed, comparing the Mg activation barriers across the different transition metal cations in our previous oxide spinel work[7] to the results presented here, we find an average ~200 meV reduction in ionic barrier, which is equivalent to ~4 orders of magnitude improvement in bulk diffusion coefficient. Beyond tuning the majority anion species, we speculate that incorporating mono-valent anions to reduce the electrostatic interaction between intercalant and host could possible improve the intercalant cation mobility. For example, theoretical calculations predict that partially substituting the O atom with F in one corner of "transition metal – oxygen" octahedron improves the Mg ion mobility for both VPO_4F and $FeSO_4F$.[19,37]. Polyanionic compounds might lead to good mobility as well, as those materials generally present a more covalent bonding framework with weaker electrostatic interactions between the host and the mobile cation.

In addition to these considerations the availability of fresh Mg near the electrode is greatly influenced by process of Mg desolvation from the bulk electrolyte followed by surface diffusion, and thus might dominate Mg bulk diffusion. [5,10,11] Previous investigation demonstrated the formation of "sturdy" ionic-couples in the electrolyte bulk and Mg desolvation energies of a multitude of electrolyte species, suggesting that the availability of fresh Mg at the surface electrodes can be largely impacted by not negligible desolvation

energies[5,10,12] proposed a desolvation mechanism of Mg electrolyte in proximity of a sulfide Cheverel cathode surface, discussing various mechanisms behind the transport of Mg from the electrode surfaces in the bulk. Wan *et al*.[5] estimated that the migration of incoming $Mg\text{-}Cl^{+}$ units from the bulk electrolyte to the surface and later into the Chevrel bulk as Mg ions only cost ~0.5 eV, hence not limiting Mg availability in the cathode bulk but manifesting *via* not negligible intercalation over-potentials at the interface.

From the synthesis viewpoint, previous research indicates that the Cr_2S_4 normal spinel framework can be prepared from their cupric compounds[38] by electrochemical removal or ion exchange of copper in certain concentration regions[39]. Normal spinel-type $Mg_xTi_2S_4$ ($0 < x < 0.5$) can also be synthesized via Mg intercalation into the cubic Ti_2S_4[40]. Indeed, recent collaborative work[31] has demonstrated that the thiospinel Ti_2S_4 shows promise as a cathode material for Mg batteries, yielding a high capacity of 195 mAh g^{-1} at an average voltage of 1.2 V at 60 °C. According to our calculations, the low energy above hull of spinel $LiMn_2S_4$ (~30meV/atom) suggests that ion exchange from the Li version could present another possible avenue for synthesis. Thus, it should be possible to test multivalent intercalation for the specific hosts identified from our computational results.

Methodology

The Vienna ab initio software package (VASP)[41] is employed to perform the density functional theory (DFT) calculations[42]. The projector augmented-wave (PAW) method is used to describe the wavefunctions near the core and the generalized gradient approximation (GGA)[43] within the Perdew–Burke–Ernzerhof (PBE)[44] parameterization is employed as the electron exchange–correlation functional. The normal spinel unit cell is used for voltage and stability calculations with the Brillouin zone sampling of 8 x 8 x 8. All

magnetic ions are initialized ferromagnetically and the cell shape, volume and atomic positions are fully optimized throughout this work[25].

We assume that the charged transition metal host framework is 'B_2S_4' and the fully discharged formula is 'AB_2S_4' across a matrix of chemical compositions spanning A = {Mg, Ca, Zn} and B = {Ti, V, Cr, Mn, Fe, Co, Ni} throughout the paper. All multivalent cathode property calculations are extracted based on the intercalation reaction of A + B_2S_4 -> AB_2S_4, unless otherwise stated. The average voltage of the intercalation reaction is calculated as[33,45]

$$\bar{V} = (E_{charge} + nE_{MV} - E_{discharge})/nz \qquad (1)$$

where E_{MV} is the energy of multivalent cation species in metal form; E_{charge} and $E_{discharge}$ are the calculated energy of the charged and discharged compounds, respectively; n is number of intercalating atoms participating in the reaction; and the z represents the oxidation state of the multivalent intercalant.

Activation barriers were calculated with the nudged elastic band (NEB) method[46]. The minimum energy paths (MEP) in the NEB procedure were initialized by linear interpolation of 8 images between the two fully relaxed endpoint geometries, and each image is converged to $<1 \times 10^{-4}$ eV per supercell. The MEPs were obtained in the dilute cation limit, i.e., one mobile species per unit cell. To ensure that fictitious interactions between the diffusing species are minimized, a 2 × 2 × 2 supercell of the primitive cell was used, for which the inter-image distance is never less than 8 Å.

We adopted a careful numerical treatment throughout this work, such as employing a constant energy cutoff for wave functions, relaxed supercells, convergence criteria wr.t. *k*-

points and total energy etc., to eliminate possible errors. The DFT methodology employed agrees well with available Mg experimental results for materials where intercalation has been well established, as shown in Tab. 2. For example, Kim *et al.* demonstrated impeded Mg intercalation in spinel MnO_2 with a voltage of 2.9V,[8] confirming our computational prediction (voltage ~2.86V, migration activation energy ~ 650-850meV)[7]; we also note that a very recent publication[31] experimentally demonstrated that Mg intercalation in *c*-TiS_2 (spinel) can yield voltage of 1.2V and capacity of 200mAh/g upon cycling because of the low migration activation energy of ~550meV, indeed confirming our predictions in this work.

We also calculated the Mg^{2+} migration in Chevrel Mo_6S_8, a well-known multivalent compound, to further demonstrate the accuracy and reliability of our calculation method. The same parameters as described above and a 2×2×2 Mo_6S_8 super cell are used to evaluate the Mg^{2+} mobility at the working ion cation dilute limit. According to previous experimental study[2,47,48], there are two types of interstitial sites in the Chevrel host structure: a stable inner site in larger cavity, and a metastable outer site in the smaller cavity (where we adopt the same name convention as defined in Levi *et al.* [2,47,48]). Mg^{2+} can reversibly intercalate into the Mo_6S_8 Chevrel host structure at a rate of C/8 and a maximum charge capacity of 135 mAh/g for several hundreds of cycles under 60°C,[1] which implies a low diffusion barrier for Mg^{2+} migrating between the inner and outer sites. As shown in Fig. 5, we found the inner site to be energetically more stable than outer site by ~200meV. Importantly, we calculated the Mg^{2+} migration energy barrier between the two sites as ~360meV along a curved path, which favors facile cation intercalation (<600meV).

Previous work focusing on interfacial Mg transport using a surface slab model of the Chevrel phase reports a theoretical energy barrier of ~500meV[11] which while higher, still

supports intercalation. To the best of our knowledge, no experimental estimations of Mg migration energy barriers exist in the literature for comparison, but the migration energy barrier of ~360meV reported here (or ~500meV elsewhere[11]) suggests good Mg^{2+} mobility, in agreement with experimental observations. [1,2,47,48] These data are incorporated into the Table 2 to facilitate comparison between calculated predictions and observed experimental intercalation.

Acknowledgements

This work was intellectually led and fully supported by the Joint Center for Energy Storage Research (JCESR), an Energy Innovation Hub funded by the U. S. Department of Energy, Office of Science, Basic Energy Sciences. Work at the Lawrence Berkeley National Laboratory was supported by the Assistant Secretary for Energy Efficiency and Renewable Energy, under Contract no. DEAC02-05CH11231. We thank Dr. Linda Nazar for useful discussions. We also thank the National Energy Research Scientific Computing Center and Argonne Leadership Computing Facility (DOE Office of Science User Facility DE-AC02-05CH11231 and DE-AC02-06CH11357) for providing computing resources. The Materials Project (BES DOE Grant no. EDCBEE) is acknowledged for infrastructure and algorithmic support.

References

1. D. Aurbach, Z. Lu, a Schechter, Y. Gofer, H. Gizbar, R. Turgeman, Y. Cohen, M. Moshkovich, and E. Levi, *Nature*, 2000, **407**, 724–7.
2. E. Levi, M. D. Levi, O. Chasid, and D. Aurbach, *J. Electroceramics*, 2007, **22**, 13–19.
3. J. Muldoon, C. B. Bucur, and T. Gregory, *Chem. Rev.*, 2014, **114**, 11683–11720.
4. H. D. Yoo, I. Shterenberg, Y. Gofer, G. Gershinsky, N. Pour, and D. Aurbach, *Energy Environ. Sci.*, 2013, **6**, 2265–2279.
5. P. Canepa, G. Sai Gautam, R. Malik, S. Jayaraman, Z. Rong, K. R. Zavadil, K. Persson, and G. Ceder, *Chem. Mater.*, 2015, **27**, 3317–3325.

6. G. Hautier, A. Jain, S. P. Ong, B. Kang, C. Moore, R. Doe, and G. Ceder, *Chem. Mater.*, 2011, **42**, 3495.
7. M. Liu, Z. Rong, R. Malik, P. Canepa, A. Jain, G. Ceder, and K. A. Persson, *Energy Environ. Sci.*, 2015, **8**, 964–974.
8. C. Kim, P. J. Phillips, B. Key, T. Yi, D. Nordlund, Y. Yu, R. D. Bayliss, S. Han, M. He, Z. Zhang, A. K. Burrell, R. F. Klie, and J. Cabana, *Adv. Mater.*, 2015, **27**, 3377.
9. Z. Rong, R. Malik, P. Canepa, G. Sai Gautam, M. Liu, A. Jain, K. A. Persson, and G. Ceder, *Chem. Mater.*, 2015, **27**, 6016.
10. N. N. Rajput, X. Qu, N. Sa, A. K. Burrell, and K. A. Persson, *J. Am. Chem. Soc.*, 2015, **137**, 3411–3420.
11. L. F. Wan, B. R. Perdue, C. A. Apblett, and D. Prendergast, *Chem. Mater.*, 2015, **27**, 5932–5940.
12. P. Canepa, S. Jayaraman, L. Cheng, N. N. Rajput, W. D. Richards, G. S. Gautam, L. A. Curtiss, K. A. Persson, and G. Ceder, *Energy Environ. Sci.*, 2015, **8**, 3718–3730.
13. R. Malik, D. Burch, M. Bazant, and G. Ceder, *Nano Lett.*, 2010, **10**, 4123–7.
14. G. Sai Gautam, P. Canepa, A. Abdellahi, A. Urban, R. Malik, and G. Ceder, *Chem. Mater.*, 2015, **27**, 3733–3742.
15. G. Sai Gautam, P. Canepa, R. Malik, M. Liu, K. Persson, and G. Ceder, *Chem. Commun.*, 2015, **51**, 13619–13622.
16. Y. Liang, R. Feng, S. Yang, H. Ma, J. Liang, and J. Chen, *Adv. Mater.*, 2011, **23**, 640–3.
17. Y. Liang, H. D. Yoo, Y. Li, J. Shuai, H. Calderon-Benavides, F. C. Robles Hernandez, L. C. Grabow, and Y. Yao, *Nano Lett.*, 2015, **15**, 2194.
18. Z.-L. Tao, L.-N. Xu, X.-L. Gou, J. Chen, and H.-T. Yuan, *Chem. Commun.*, 2004, 2080–2081.
19. A. Emly and A. Van der Ven, *Inorg. Chem.*, 2015, **54**, 4394.
20. M. M. Thackeray, P. G. Bruce, J. B. Goodenough, and S. P. Road, *Mat. Res. Bull.*, 1983, **18**, 461–472.
21. M. M. Thackeray, L. a. de Picciotto, a. de Kock, P. J. Johnson, V. a. Nicholas, and K. T. Adendorff, *J. Power Sources*, 1987, **21**, 1–8.
22. J. Bhattacharya and A. Van der Ven, *Phys. Rev. B*, 2010, **81**, 104304.
23. S. Okamoto, T. Ichitsubo, T. Kawaguchi, Y. Kumagai, F. Oba, S. Yagi, K. Shimokawa, N. Goto, T. Doi, and E. Matsubara, *Adv. Sci.*, 2015, **2**, 1500072.
24. M. M. Thackeray, *J. Electrochem. Soc.*, 1992, **139**, 363.
25. A. Jain, S. P. Ong, G. Hautier, W. Chen, W. D. Richards, S. Dacek, S. Cholia, D. Gunter, D. Skinner, G. Ceder, and K. a. Persson, *APL Mater.*, 2013, **1**, 011002.
26. S. P. Ong, L. Wang, B. Kang, and G. Ceder, *Chem. Mater.*, 2008, **77**, 1798–1807.
27. S. P. Ong, A. Jain, G. Hautier, B. Kang, and G. Ceder, *Electrochem. commun.*, 2010, **12**, 427–430.
28. A. Jain, G. Hautier, S. P. Ong, C. J. Moore, C. C. Fischer, K. a. Persson, and G. Ceder, *Phys. Rev. B*, 2011, **84**, 045115.
29. J. C. Kim, X. Li, C. J. Moore, S. H. Bo, P. G. Khalifah, C. P. Grey, and G. Ceder, *Chem. Mater.*, 2014, **26**, 4200–4206.
30. L. Pauling, *J. Am. Chem. Soc.*, 2000, **51**, 1010–1026.
31. X. Sun, P. Bonnick, V. Duffort, M. Liu, G. Ceder, and L. F. Nazar, *Energy Environ.*

Sci.
32. I. D. Brown, *Acta Crystallogr. Sect. B Struct. Sci.*, 1988, **44**, 545–553.
33. M. Aydinol, a. Kohan, G. Ceder, K. Cho, and J. Joannopoulos, *Phys. Rev. B*, 1997, **56**, 1354–1365.
34. *Online Suppl. Inf.*
35. F. Beck and P. Rüetschi, *Electrochim. Acta*, 2000, **45**, 2467–2482.
36. H. Gwon, S. W. Kim, Y. U. Park, J. Hong, G. Ceder, S. Jeon, and K. Kang, *Inorg. Chem.*, 2014, **53**, 8083–8087.
37. J. Wu, G. Gao, G. Wu, B. Liu, H. Yang, X. Zhou, and J. Wang, *RSC Adv.*, 2014, **4**, 15014.
38. R. E. Tressler, F. a Hummel, and V. S. Stubican, *J. Am. Ceram. Soc.*, 1968, **51**, 648–651.
39. V. Bodenez, L. Dupont, L. Laffont, a. R. Armstrong, K. M. Shaju, P. G. Bruce, and J.-M. Tarascon, *J. Mater. Chem.*, 2007, **17**, 3238.
40. P. Lightfoot, F. Krok, J. L. Nowinski, and P. G. Bruce, *J. Mater. Chem*, 1992, **2**, 139–140.
41. G. Kresse and J. Furthmüller, *Phys. Rev. B. Condens. Matter*, 1996, **54**, 11169–11186.
42. W. Kohn and L. J. Sham, *Phys. Rev.*, 1965, **140**, A1133.
43. J. P. Perdew, K. A. Jackson, M. R. Pederson, D. J. Singh, and C. Fiolhais, *Phys. Rev. B*, 1992, **46**.
44. J. Perdew, K. Burke, and M. Ernzerhof, *Phys. Rev. Lett.*, 1996, **77**, 3865–3868.
45. M. K. Aydinol and G. Ceder, *J. Electrochem. Soc.*, 1997, **144**, 1–4.
46. G. Henkelman, B. P. Uberuaga, and H. Jonsson, *J. Chem. Phys.*, 2000, **113**, 9901–9904.
47. E. Levi, E. Lancry, a Mitelman, D. Aurbach, G. Ceder, D. Morgan, and O. Isnard, *Chem. Mater.*, 2006, **18**, 5492–5503.
48. E. Levi, E. Lancry, A. Mitelman, D. Aurbach, O. Isnard, and D. Djurado, *Chem. Mater.*, 2006, **18**, 3705–3714.
49. https://materialsproject.org/batteries/mvc-1200677217/

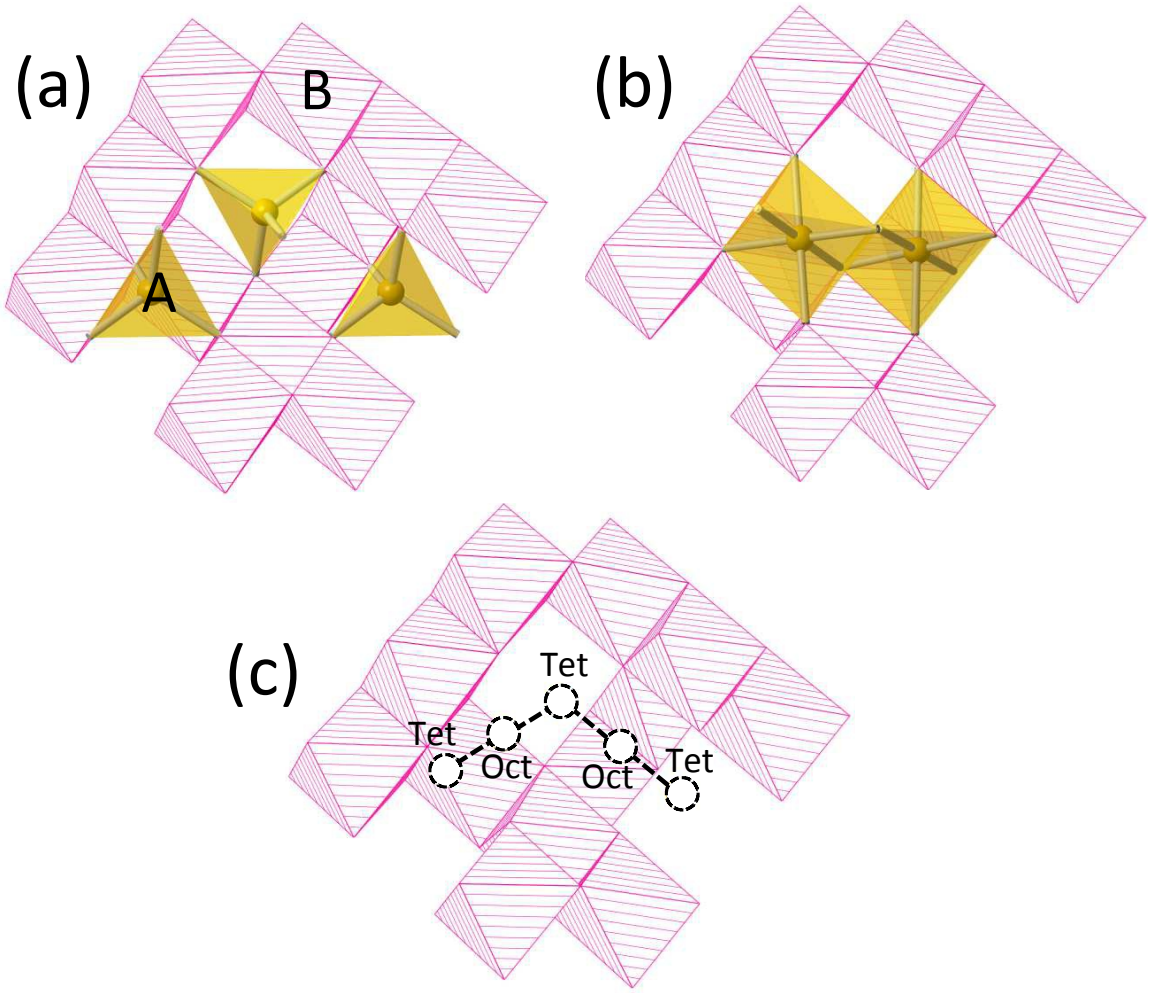

Figure 1. In AB_2X_4 spinel crystal structures, the 'A' atom (yellow polyhedra) can occupy either the (a) tetrahedral site or (b) octahedral site. When the 'A' atom diffuses through the spinel host structure framework (pink octahedrons built with 'B' and S atoms), it alternates between the tetrahedral site and octahedral site along a (c) zigzag energy minimum path.

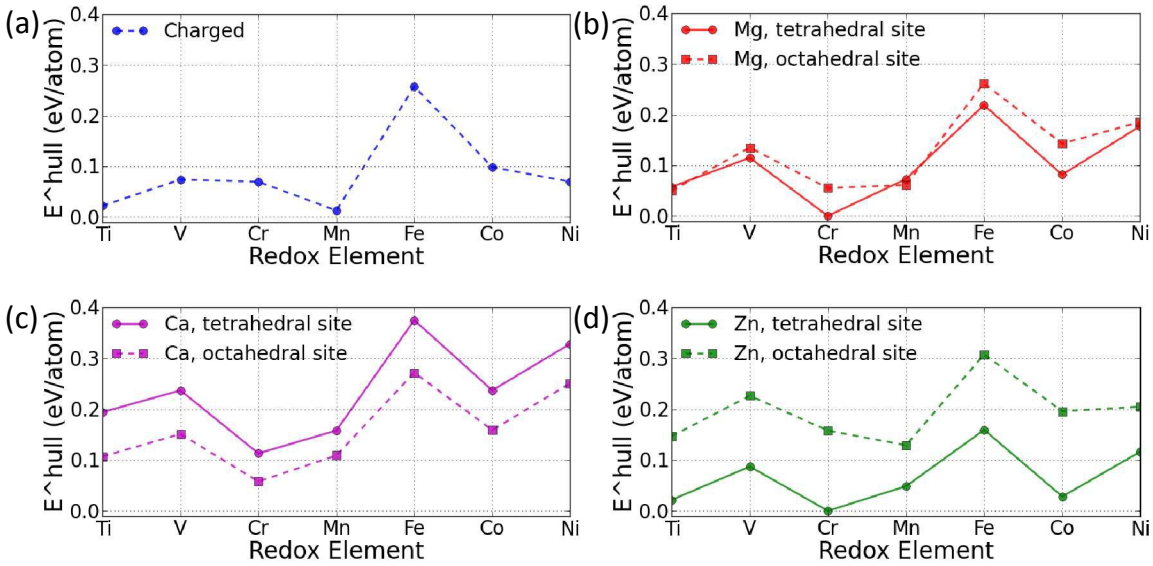

Figure 2. The calculated thermodynamic stabilities of sulfur spinel compounds in the (a)charged and (b-d)discharged phases. The energy above hull is measured as the formation energy difference between a compound and the convex hull formed by stable compounds. The distance between the dashed and solid lines indicate site energy preferences for the cation in the discharged state.

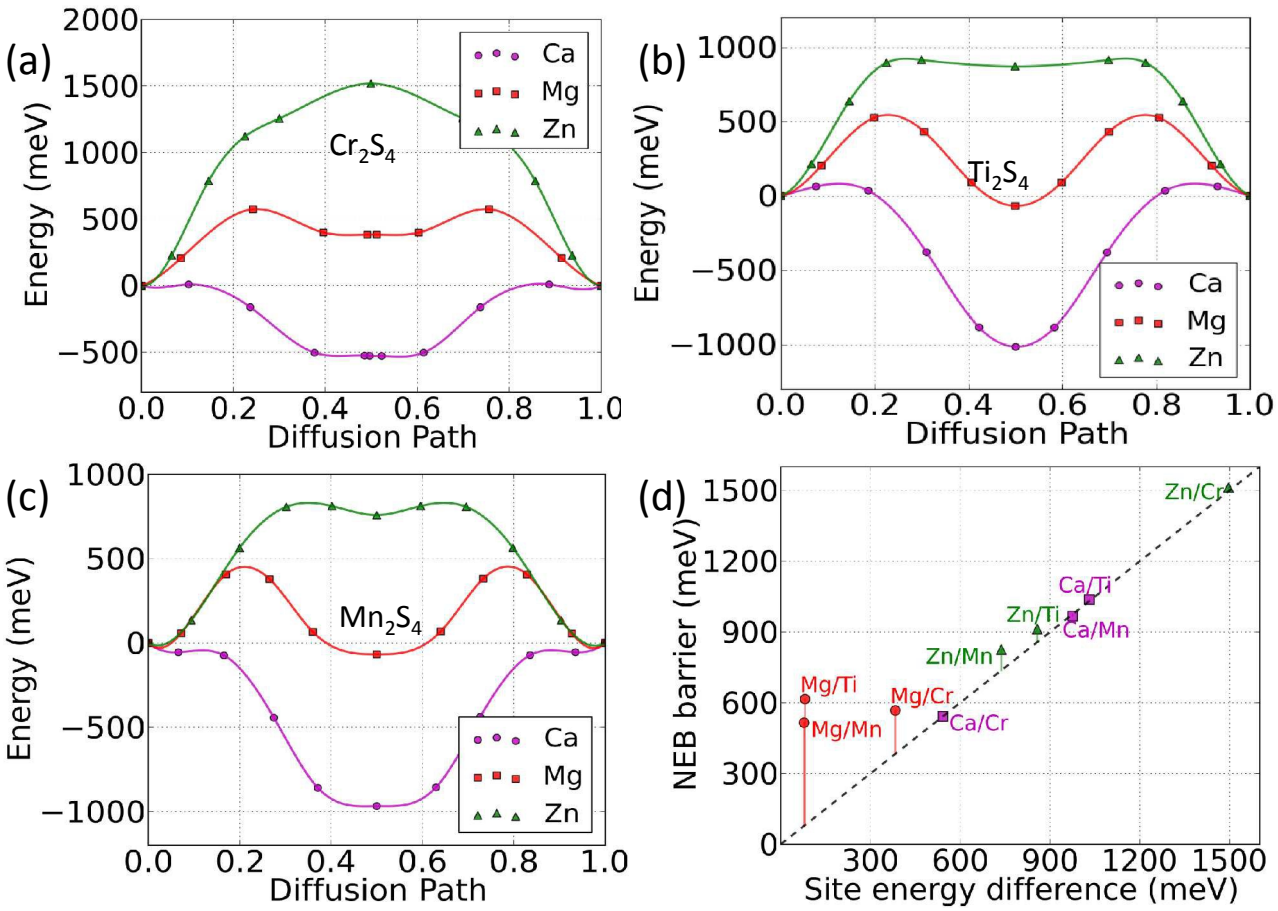

Figure 3. Calculated energy barrier for migration of 'A' cation in spinel along the minimum energy path as obtained by first-principles nudged elastic band (NEB) in calculations. (a)Cr_2S_4, (b)Ti_2S_4 and (c)Mn_2S_4 within dilute limit of cation insertion . (d) The correlation between site energy difference of the cation (see Figure 2) and the NEB migration barrier.

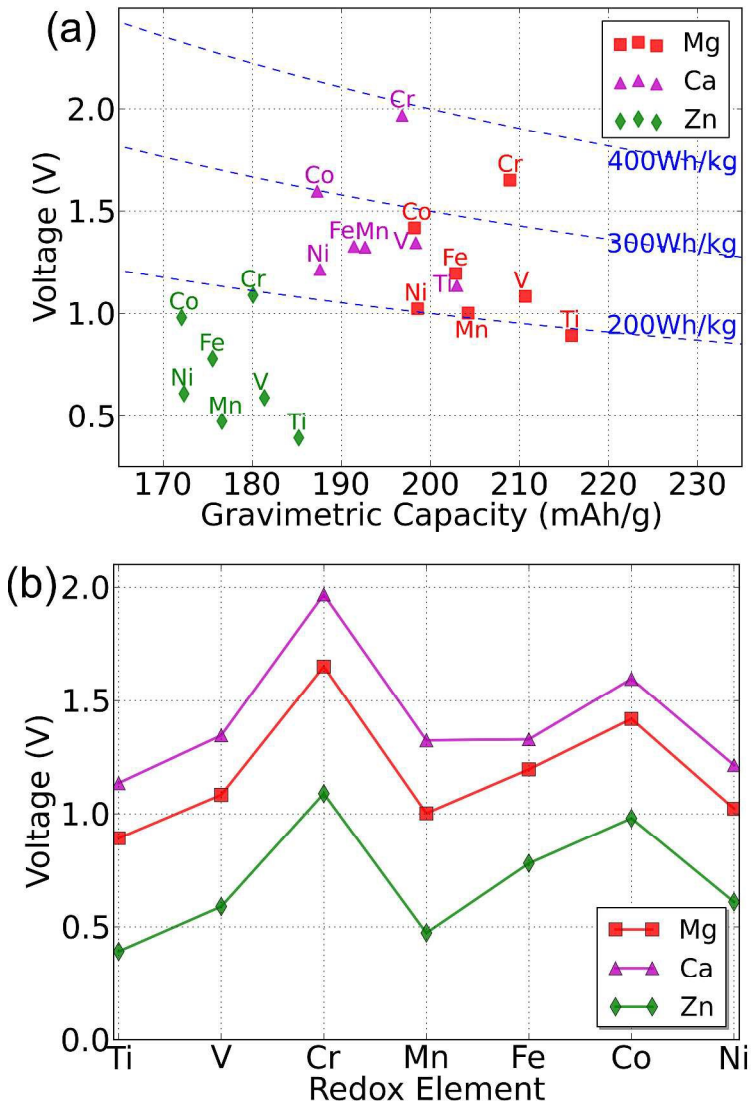

Figure 4. (a) The calculated average voltage vs. gravimetric capacity for intercalation of 'A' = {Zn, Ca, Mg} in B_2S_4 spinels up to composition AB_2S_4. The redox-active metal is marked next to each point for clarification. Dashed curves are plotted to mark the specific energy of 200 Wh/kg, 300 Wh/kg and 400 Wh/kg as reference values, respectively. (b) The calculated voltage of each spinel phase as a function of the redox-active transition metal and intercalating cation. The different colors denote different intercalating species as specified by the legend.

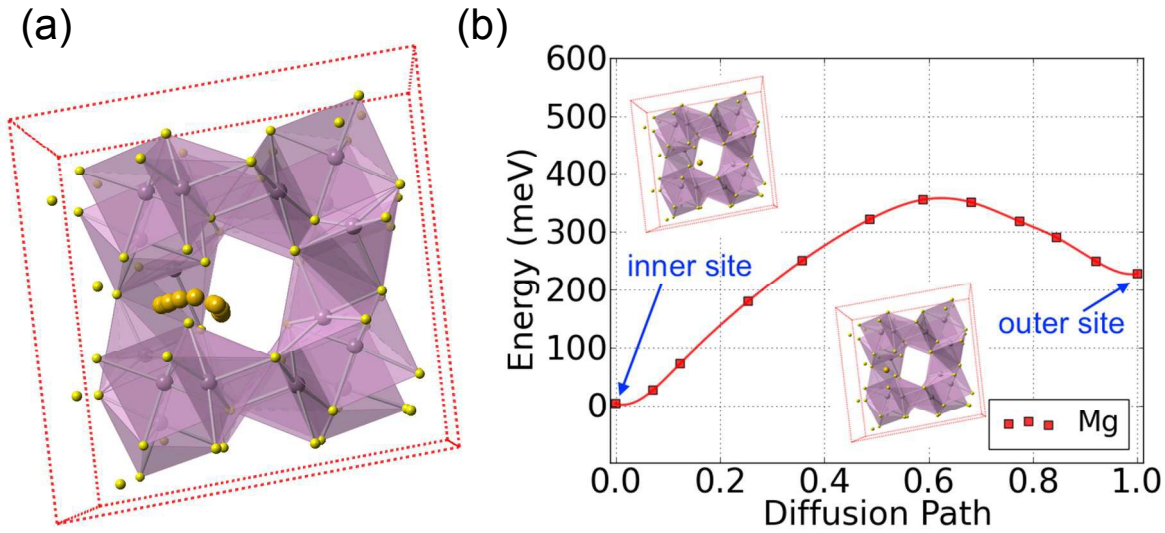

Figure 5. (a) The Mg^{2+} migration path in the Chevrel Mo_6S_8 phase between the inner and outer sites; (b) the migration energy of Mg^{2+} in Mo_6S_8 along the lowest energy path based on the first-principles nudged elastic band method.

Table 1. Properties of selected multivalent sulfur spinel systems.

Spinel Materials	Stable 'A' site	Voltage (V)	Capacity (mAh/g)	Diffusion Barrier (meV)
Mg in Cr_2S_4	Tet	1.65	209	542
Mg in Ti_2S_4	Oct	0.89	216	615
Mg in Mn_2S_4	Oct	1.00	204	515
Ca in Cr_2S_4	Oct	2.16	197	567

Table 2. Comparison between theory and experiment from previous studies. The DFT evaluated properties are in good agreement with experimental values vs. Mg^{2+}/Mg^{0}.

Material system	Average Voltage (theory)	Average Voltage (expt.)	Migration activation energy (theory)	Migration activation energy (expt.)
Spinel MnO_2	2.86 V [7]	2.9 V [8]	650–850 meV [7]	Impeded [8]
Spinel TiS_2	0.89 V(this work)	1.2 V [31]	615 meV(this work)	550 meV [31]
Chevrel Mo_6S_8	0.99 V [49]	1-1.3 [1,11]	~360 meV(this work) ~500 meV[11]	Operable C/8 [1]